Peripapillary Choroidal Vascularity Index in Glaucoma—A Comparison Between Spectral-Domain OCT and OCT Angiography

Jun Woo Park,[1] Min Hee Suh,[1] Rupesh Agrawal,[2–4] and Neha Khandelwal[2–4]

[1]Department of Ophthalmology, Haeundae Paik Hospital, Inje University College of Medicine, Busan, South Korea
[2]Singapore Eye Research Institute, Singapore National Eye Center, Singapore, Republic of Singapore
[3]National Healthcare Group Eye Institute, Department of Ophthalmology, Tan Tock Seng Hospital, Singapore, Republic of Singapore
[4]Nanyang Technology University, Singapore, Republic of Singapore

Correspondence: Min Hee Suh, Department of Ophthalmology, Haeundae Paik Hospital, Inje University College of Medicine, 1435 Jwa-dong, Haeundae-gu, Busan 612-030, South Korea;
crishuna6@gmail.com.

Submitted: March 16, 2018
Accepted: June 6, 2018

Citation: Park JW, Suh MH, Agrawal R, Khandelwal N. Peripapillary choroidal vascularity index in glaucoma—a comparison between spectral-domain OCT and OCT angiography. *Invest Ophthalmol Vis Sci*. 2018;59:3694–3701. https://doi.org/10.1167/iovs.18-24315

Purpose. To compare the choroidal vascularity index (CVI) determined by spectral-domain optical coherence tomography (OCT) between eyes with and without parapapillary deep-layer microvasculature dropout (MvD_P) assessed by OCT angiography in glaucomatous eyes.

Methods. A total of 100 open-angle glaucoma patients with and without MvD_P (50 eyes of 50 patients in each group) matched by age and visual field mean deviation were included. Total choroidal area (TCA) and CVI were measured by image binarization of spectral-domain OCT B-scans in order to assess the choroidal vasculature outside β-zone parapapillary atrophy (βPPA) at a 3.5-mm distance from the Bruch's membrane opening center. MvD_P was determined by OCT angiography as a deep-layer microvasculature dropout within βPPA. Global and sectoral (six 60° sectors) TCA and CVI were compared between eyes with and without MvD_P.

Results. The CVIs of eyes with MvD_P were significantly lower than those without MvD_P, globally ($P = 0.010$) as well as in the inferotemporal (TI) ($P = 0.003$), temporal ($P = 0.009$), and nasal ($P = 0.048$) sectors. Eyes with MvD_P, of which the largest portion was located only in the TI sector ($n = 33$), had significantly lower CVI than those without MvD_P in the corresponding TI and temporal sectors ($P < 0.05$ for all), whereas TCA did not differ in any areas.

Conclusions. Eyes with MvD_P had significantly lower CVIs than did those without MvD_P. Furthermore, CVI reduction was spatially correlated with MvD_P. Further studies investigating the influence of MvD_P on the choroidal vasculature outside βPPA are warranted.

Keywords: choroidal vascularity index, OCT angiography, deep-layer microvasculature dropout, CVI, OCTA

Although glaucoma is a multifactorial disease, a potential pathogenic role of ocular blood flow or microvasculature in the development and progression of glaucomatous optic neuropathy has long been recognized.[1,2] Recently, parapapillary deep-layer microvasculature dropout (MvD_P) has been observed with the complete dropout of the choriocapillaris or microvasculature within the sclera in β-zone parapapillary atrophy (βPPA) by optical coherence tomography angiography (OCT-A).[3–5] MvD_P has been reported to be associated with glaucomatous visual field (VF) damage and focal lamina cribrosa (LC) defect.[3,6]

However, the relationship between MvD_P and choroidal thickness is controversial,[3,7] and the literature on the association of the choroidal vasculature outside the βPPA with MvD_P is limited. The conventional imaging method, indocyanine green angiography (ICG), is both invasive and of limited utility for visualization of the vasculature in a segmented layer[4]; OCT-A, moreover, is limited in its evaluation of the vasculature outside the βPPA, due to projection artifacts from the highly reflective deep vasculature within the retinal pigment epithelium (RPE).[3,8] Although choroidal thickness may serve as a surrogate for the choroidal vasculature, direct measurement of the choroidal vasculature outside the βPPA and its comparison with the MvD_P is needed in order to elucidate the relationship between those two adjacent vascular structures.

Recently, in vivo quantification of the choroidal vasculature outside the βPPA based on the reflectivity of the choroidal structure as imaged by spectral-domain OCT (SD-OCT) was newly introduced.[9–17] Specifically, there are a number of reports regarding the clinical relevance of the choroidal vascularity index (CVI) for various retinal diseases.[9,11–16]

The purpose of the present study was to determine the total choroidal area (TCA) and CVI by means of image binarization of SD-OCT images and to compare them between glaucomatous eyes with and without OCT-A-determined MvD_P.

Methods

This study included primary open angle glaucoma (POAG) patients who had visited the Haeundae Paik Hospital Glaucoma Clinic between January and September 2017. It was approved by the Institutional Review Board of Haeundae Paik Hospital and all procedures adhered to the tenets of the Declaration of Helsinki. Informed consent was obtained from all of the subjects.

Study Subjects

All of the POAG patients enrolled for this study had good-quality OCT-A and optic nerve head (ONH) images obtained by SD-OCT. All underwent an ophthalmic examination, including measurement of best-corrected visual acuity, refraction, slit-lamp biomicroscopy, intraocular pressure (IOP) measurement by Goldmann applanation tonometry, gonioscopy, central corneal thickness (CCT) measurement with the Pentacam Scheimpflug imaging system (Oculus Optikgeräte GmbH, Wetzlar, Germany), axial length measurement by IOL Master (Carl Zeiss Meditec, Dublin, CA, USA), dilated fundus examination, simultaneous color and red-free fundus photography (TRC-NW8; Topcon, Tokyo, Japan), standard automated perimetry (SAP) (Humphrey Field Analyzer; 30-2 Swedish interactive threshold algorithm; Carl-Zeiss Meditec), SD-OCT, and OCT-A (Spectralis; Heidelberg Engineering GmbH, Heidelberg, Germany). Standard automated perimetry and all of the imaging tests were performed within a 6-month period. Systolic and diastolic blood pressure (BP) were measured at the height of the heart with an automatic BP-measurement instrument (Model Easy X 800 [R/L]; DAWON Medical Co. Ltd., Kungsan, Korea). Mean arterial pressure was calculated as ⅓ systolic BP + ⅔ diastolic BP, and mean ocular perfusion pressure was calculated as the difference between ⅔ of the mean arterial pressure and the IOP.[3] An optic disc hemorrhage was defined as an isolated flame-shaped or splinter hemorrhage on the ONH based on regular optic disc examinations or standardized review of fundus photographs performed approximately every 6 months.

For inclusion in this study, the POAG patients were required to have visible βPPA of a temporal width ≥100 μm on fundus photographs of at least one radial scan measured by the built-in caliper of SD-OCT, and best-corrected visual acuity ≥20/40.[3] Subjects with a history of ocular surgery (except for uncomplicated cataract or glaucoma surgery), intraocular diseases other than glaucoma (e.g., diabetic retinopathy or nonglaucomatous optic neuropathy) or systemic diseases (e.g., stroke or pituitary tumor) that could influence the study results were excluded.[3] Those with an unreliable VF or poor-quality imaging tests also were excluded.[3] Those with diabetes mellitus and systemic hypertension were included unless they had been diagnosed with diabetic or hypertensive retinopathy.[3]

POAG was defined as the presence of glaucomatous optic nerve damage (i.e., the presence of focal thinning, notching, and localized or diffuse atrophy of the retinal nerve fiber layer [RNFL]) and compatible repeated VF damage and open angles on gonioscopy. Glaucomatous VF damage was defined as a VF outside the normal limits on the glaucoma hemifield test or a pattern standard deviation outside 95% normal limits, as confirmed on two consecutive, reliable (≤33% fixation losses and false negatives, ≤15% false positives) tests.[3]

OCT-A Imaging

The Spectralis OCT Angiography Module (Spectralis; Heidelberg Engineering GmbH) incorporated into the OCT2 platform provides the noninvasive visualization of the vascular structures of various user-defined retinal layers. Details on the Spectralis OCT-A is described elsewhere.[18] Briefly, this technology has an acquisition speed of 85 kHz, a central wavelength of 880 nm, and lateral and axial resolutions of 5.7 μm and 3.9 μm per pixel, respectively. In this study, the 15° × 10° scan pattern was used to acquire scans consisting of 256 clusters of 5 repeated B-scans. Based on a review by two interpreters (MHS and JWP), OCT-A images judged to be of poor quality according to the following criteria were excluded: (1) quality score <25, (2) poor clarity, (3) residual motion artifacts visible as irregular vessel pattern or disc boundary on enface angiogram, (4) local weak signal, and (5) choroidal-layer segmentation errors.[3]

Dropout of Deep-Layer Microvasculature in Parapapillary Atrophy

Details on the determination of MvD_P can be found elsewhere.[3] Briefly, two independent observers (MHS and JWP) masked to the patients' optic disc features and other characteristics determined MvD_P as complete dropout of the choriocapillaris or microvasculature contained in the scleral flange within the βPPA on both horizontal and enface OCT-A vessel-density maps (Figs. 1A3, 1B3). MvD_P was required to be present on at least four consecutive horizontal B-scans and to be ≥200 μm in diameter on at least one scan.[3] MvD_P location was determined based on the six sectors extending from a fovea-Bruch's membrane opening (BMO) axis, the angles of which were 45° for the superotemporal (TS), inferotemporal (TI), superonasal (NS), and inferonasal (NI) sectors and 90° for the nasal (N) and temporal (T) sectors (Figs. 1A3, 1A4, 1B3, 1B4). If the subject had MvD_P located in ≥2 neighboring sectors, the sector that included the largest portion of the MvD_P was assigned.[3] Discrepancies between the two interpreters were resolved by consensus or if consensus could not be reached, the subject was excluded from the analysis.[3] If both eyes of an POAG patient had MvD_P or did not have MvD_P, one eye was randomly enrolled. If a patient had one eye with and one eye without MvD_P, the eye with MvD_P was included. In order to minimize the effects of glaucoma severity and age on MvD_P and CVI, glaucomatous eyes having MvD_P were matched (by the individual matching method) to those not having MvD_P for VF mean deviation (MD) and age.

SD-OCT Imaging

Spectralis OCT2 Glaucoma Module Premium Edition software (version 1.9.17.0; Heidelberg Engineering GmbH) offers 24 consecutive radial B-scans and an ONH radial circle scan pattern that are aligned according to the fovea-to-BMO center axis. This scan pattern was used to determine RNFL thicknesses, the βPPA microstructure, BMO area, fovea-BMO angle, TCA, and CVI. Circumpapillary RNFL thickness was calculated at each point on a set-diameter (3.5 mm) circle in a global area as well as in the six sectors. βPPA was defined as the area without the RPE, and βPPA_{-BM} was defined as the area with an exposed Elschnig's ring between the optic disc boundary and the BMO.[3] Focal LC defects defined as laminar holes or laminar disinsertions violating the normal U- or W-shaped contour of the anterior laminar surface were determined by the two masked independent observers (MHS and HRK) by using a 20° × 20° high-resolution scan pattern that included 48 radial B-scans in the enhanced depth imaging mode.[6,19,20] Subjects were excluded in cases of failure to reach consensus between the two observers.

Investigative Ophthalmology & Visual Science

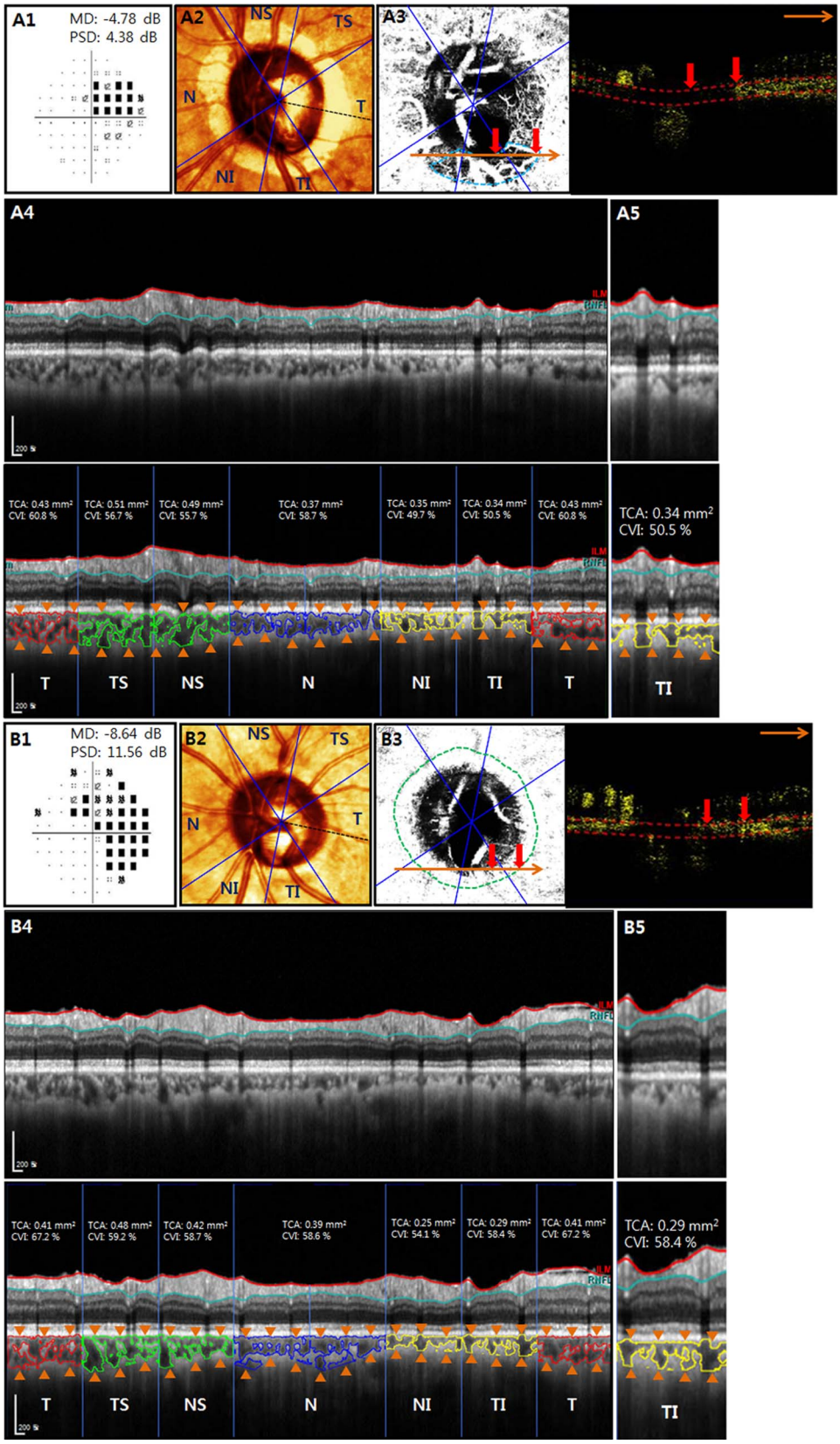

Figure 1. SD-OCT-derived CVI for POAG patients with and without OCT-A-derived MvD_P. Left eye of 73-year-old male with MvD_P (**A**), and left eye of 69-year-old male without MvD_P (**B**). (**A1**, **B1**) The eye with MvD_P had better VF MD and pattern standard deviation (**A1**) than those of the eye without MvD_P (**B1**). (**A2**, **B2**) On SD-OCT scanning laser ophthalmoscopy images, six sectors extending from the fovea-BMO axis (*black dotted lines*), the angles of which were 45° for the TS, TI, NS, and NI sectors and 90° for the N and T sectors, were divided for assessment of the MvD_P and CVI. (**A3**, **B3**) Note that the eye with MvD_P had complete dropout of the choriocapillaris mainly in the TI sector (*sky-blue dotted lines* and *red arrows*) (**A3**), whereas the eye without MvD_P had a preserved choriocapillaris within the βPPA (*green dotted lines* and *red arrows*) (**B3**) on both

enface (*left*) and horizontal (*right*) OCT-A images. The large *orange arrowheads* indicate the locations of a horizontal B-scan. (**A4**, **B4**) CVI was derived by dividing an area of dark pixels suggestive of choroidal vasculature (*bald solid lines*) by the TCA (*orange arrowheads*). A reduced CVI of the eye with MvD_P was noted in all six sectors, with the largest difference in the TI sector (**A4**), relative to the eye without MvD_P (**B4**), whereas the TCA did not show any noticeable differences between the two eyes (**A4**, **B4**). (**A5**, **B5**) Higher magnification of the TI sector showed the reduced CVI of the eye with MvD_P (**A5**) relative to the eye without MvD_P (**B5**).The *bottom* images of A4, A5, B4, and B5 are the same as the *top* images but contain labels explaining the choroidal vasculature.

Measurement of CVI and TCA

CVI and TCA were measured based on the 3.5-mm-sized ONH radial circle scan of the Spectralis OCT2 Glaucoma Module Premium Edition software. Details on the measurement of TCA and CVI are available elsewhere.[9,11,14] Briefly, the scanned image was segmented according to a modified version of the protocol described by Sonoda et al.[21,22] Image binarization was performed using public domain software, ImageJ (version 1.47; available in the public domain, https://imagej.net/Citing), which can convert gray-scale images to binarized images. Niblack's[23] autolocal threshold techniques were used for image binarization.[9,11–14] The choroidal area was defined as the area between the upper border marked at the RPE and the lower border of light pixels at the choroid scleral junction (Figs. 1A4, 1A5, 1B4, 1B5). Then, the image was converted to red, green, and blue color to allow the color threshold tool to select the dark pixels,[9] and the TCA was calculated as the area between the RPE and the choroid scleral junction (Figs. 1A4, 1A5, 1B4, 1B5). The luminal area (LA) was defined as the vascular area of dark pixels within the choroid. To determine the choroidal vascularity, the CVI was computed by dividing the LA by the

Table 1. Comparison of the Demographics and Test Results Between POAG Patients According to the Presence of MvD_P

Variables	Eyes With MvD_P (n = 50)	Eyes Without MvD_P (n = 50)	P Value
Age, y	56.4 ± 14.9	54.6 ± 16.6	0.596*
Sex, male/female	25/25	28/22	0.550†
Spherical equivalent, D	−3.4 ± 4.0	−2.4 ± 3.6	0.128*
Axial length, mm	25.2 ± 1.9	25.2 ± 1.8	0.932*
CTT, μm	532.3 ± 36.3	534.2 ± 37.3	0.826‡
Self-reported diabetes, n (%)	4 (8.0)	7 (14.0)	0.340†
Self-reported HT, n (%)	8 (16.0)	11 (22.0)	0.447†
Diabetes medication, n (%)	4 (8.0)	7 (14.0)	0.340†
Antihypertensive medication, n (%)	8 (16.0)	11 (22.0)	0.447†
Number of topical glaucoma medications, n (%)			0.562†
0	4 (8.0)	2 (4.0)	
1	8 (16.0)	11 (22.0)	
>1	38 (76.0)	37 (74.0)	
Topical medications, n			0.690†
Prostaglandin analogs	33	24	
Beta-antagonists	35	32	
Carbonic anhydrase inhibitors	32	36	
Alpha-1-agonists	18	17	
Baseline IOP, mm Hg	17.9 ± 6.2	18.3 ± 6.3	0.946*
IOP at the time of the testing, mm Hg	12.3 ± 3.0	12.2 ± 2.8	0.628*
Systolic BP, mm Hg	122.0 ± 13.8	121.6 ± 13.1	0.893‡
Diastolic BP, mm Hg	74.0 ± 10.2	74.0 ± 10.7	0.982‡
MOPP, mm Hg	48.2 ± 10.3	46.3 ± 7.2	0.624*
Presence of βPPA_{-BM}, n (%)	25 (50.0)	27 (54.0)	0.690†
Disc hemorrhage, n (%)	7 (14.0)	4 (8.0)	0.338†
VF MD, dB	−6.1 ± 5.1	−6.1 ± 5.4	0.858*
VF PSD, dB	7.0 ± 4.1	6.1 ± 3.5	0.352*
RNFL thickness, μm			
Global area	71.3 ± 13.7	73.9 ± 13.6	0.264‡
T	58.7 ± 15.5	63.6 ± 12.7	0.073‡
TS	90.0 ± 36.6	97.4 ± 35.6	0.324‡
NS	94.3 ± 26.3	92.3 ± 27.8	0.656‡
N	65.5 ± 17.8	63.0 ± 16.8	0.447‡
NI	77.8 ± 26.1	81.4 ± 22.6	0.456‡
TI	66.9 ± 30.1	71.4 ± 29.2	0.173‡
Focal LC defect, n (%)	26 (52.0)	14 (28.0)	**0.015**†
BMO area, mm^2	2.7 ± 0.9	2.2 ± 0.4	**<0.001**‡
Foveal-BMO angle, °	−6.7 ± 3.6	−7.4 ± 3.4	0.182‡
Time of the SD-OCT, h	13:00 ± 02:24	13:42 ± 02:06	0.185*

Values are shown in mean ± standard deviation. Statistically significant values are shown in bold. HT, systemic hypertension; MOPP, mean ocular perfusion pressure; PSD, pattern standard deviation.

* The comparison was performed with Mann-Whitney test.

† The comparison was performed with chi-squared test.

‡ The comparison was performed with independent samples t-test.

Table 2. Comparison of the TCA and CVI Measured by SD-OCT Between Eyes With and Without MvD_P

Variables	Eyes With MvD_P ($n = 50$)	Eyes Without MvD_P ($n = 50$)	*P* Value*
CVI, %			
Global area	60.76 ± 4.22	62.95 ± 4.30	**0.012***
T	62.05 ± 6.20	65.03 ± 5.98	**0.016***
TS	61.67 ± 6.14	62.71 ± 5.11	0.360*
NS	60.01 ± 5.05	61.25 ± 4.49	0.197*
N	61.10 ± 4.34	63.09 ± 5.09	**0.038***
NI	59.50 ± 5.11	61.48 ± 6.07	0.082*
TI	59.43 ± 5.15	62.39 ± 5.37	**0.006***
TCA, mm^2			
Global area	3.45 ± 1.27	3.90 ± 1.04	**0.016†**
T	0.79 ± 0.33	0.89 ± 0.27	**0.043†**
TS	0.46 ± 0.19	0.52 ± 0.15	**0.023†**
NS	0.48 ± 0.20	0.54 ± 0.15	**0.027†**
N	0.93 ± 0.35	1.05 ± 0.30	**0.038†**
NI	0.38 ± 0.13	0.44 ± 0.13	**0.008†**
TI	0.36 ± 0.14	0.41 ± 0.13	**0.014†**

Values are shown in mean ± standard deviation. Statistically significant values are shown in bold.

* The comparison was performed with independent samples *t*-test.

† The comparison was performed with Mann-Whitney test.

TCA (Figs. 1A4, 1A5, 1B4, 1B5). The CVI and TCA were derived from the global area and the six sectors corresponding to those used to determine the location of MvD_P on OCT-A (Figs. 1A3, 1A4, 1B3, 1B4).

Data Analysis

The baseline characteristics, RNFL thickness, VF MD, PSD, TCA, and CVI were compared between the POAG eyes with and without MvD_P. An independent samples *t*-test was performed for normally distributed variables, a Mann-Whitney test for continuous nonnormal variables, and chi-squared test for categoric variables. A linear regression analysis was performed to evaluate the relationship of the CVI to the TCA and VF MD, PSD, and RNFL thickness. To evaluate the interobserver agreement on determination of the MvD_P, βPPA_{-BM}, and focal LC defect, the Kappa coefficient was calculated. All of the statistical analyses were performed with MedCalc (MedCalc, Inc., Mariakerke, Belgium). The α level (type I error) was set at 0.05.

Results

Two hundred and twenty-four eyes of 213 consecutive POAG patients who had been evaluated for eligibility were included in this report. Among them, 37 were excluded for the following reasons: (1) poor quality SD-OCT images ($n = 6$), (2) poor quality OCT-A images ($n = 8$), (3) failure to reach interobserver consensus in determination of focal LC defect ($n = 9$) and/or MvD_P ($n = 6$), and (4) unreliable VF results ($n = 10$). Among the remaining 187 eyes, 50 eyes of 50 POAG patients were included in each group after matching VF MD and age between patients with and without MvD_P. The interobserver agreements for the determination of the presence of MvD_P, focal LC defect, and βPPA_{-BM} were excellent (Kappa, 0.89; 95% CI, 0.84–0.98; $P < 0.001$ for MvD_P; Kappa, 0.87; 95% CI, 0.83–0.90; $P < 0.001$ for focal LC defect; and Kappa, 0.86; 95% CI, 0.75–0.98; $P < 0.001$ for βPPA_{-BM}).

The clinical characteristics of the study subjects are provided in Table 1. Eyes with and without MvD_P did not differ by age, axial length, VF MD or PSD, presence of βPPA_{-BM}, time of SD-OCT scan, IOP, or disc hemorrhage ($P > 0.05$). Meanwhile, eyes with MvD_P showed a significantly higher prevalence of focal LC defects (52.0% vs. 28.0%; $P = 0.015$) and a larger BMO area (2.5 ± 0.8 mm^2 vs. 2.1 ± 0.5 mm^2; $P = 0.003$) than those without MvD_P.

Table 2 lists the CVI and TCA data according to the presence of MvD_P. Eyes with MvD_P had a significantly lower CVI than those without MvD_P in the global area (60.76% ± 4.22% vs. 62.95% ± 4.30%; $P = 0.010$) as well as in the TI (59.43% ± 5.15% vs. 62.39% ± 5.37%; $P = 0.003$), T (62.05%

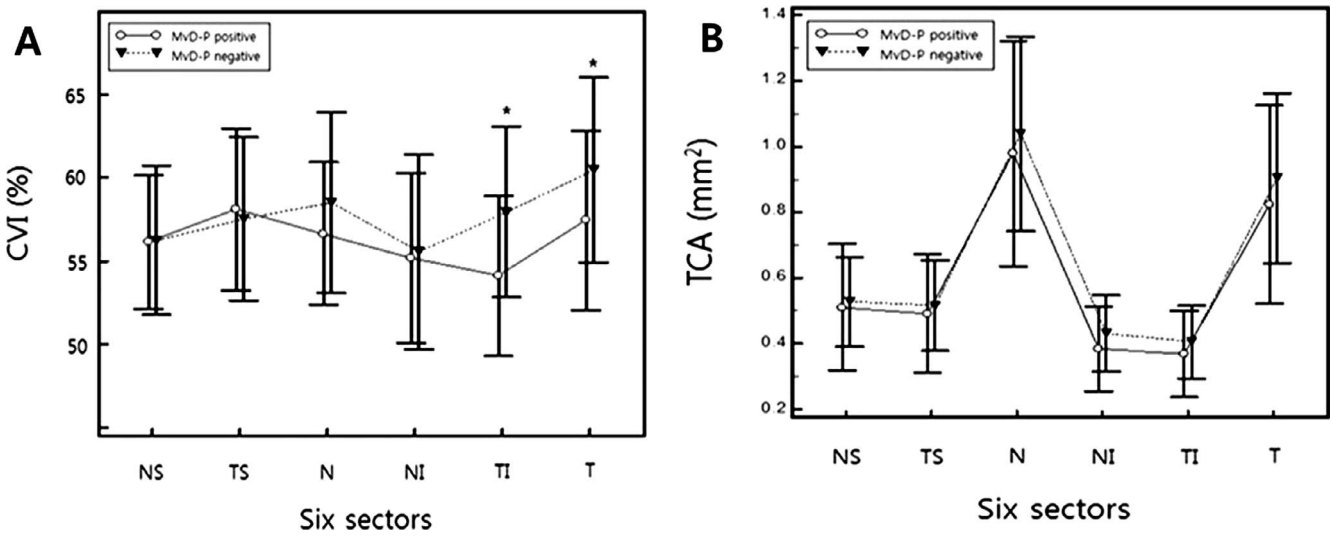

Figure 2. Comparison of CVI (**A**) and TCA (**B**) profiles between glaucomatous eyes with and without deep-layer microvasculature dropout (MvD_P). (**A**) Subset of 33 eyes with MvD_P, of which the largest portion was located only in the TI sector, had a significantly lower CVI in the TI and T sectors compared with those without MvD_P. The sector differences were greatest in the TI sector. (**B**) The TCA of the two subgroups did not differ in any sector. Each *error bar* represents the mean ± 1 SD.

Table 3. Linear Regression Analysis Between the CVI and TCA in Eyes With and Without MvD_P

	Eyes With MvD_P ($n = 50$)			Eyes Without MvD_P ($n = 50$)		
Variables	Equation	r^2	P	Equation	r^2	P
Global area	$y = 0.025\ x + 0.52$	0.57	<0.001	$y = 0.030\ x + 0.51$	0.52	<0.001
T	$y = 0.13\ x + 0.52$	0.44	<0.001	$y = 0.16\ x + 0.51$	0.50	<0.001
TS	$y = 0.19\ x + 0.53$	0.33	<0.001	$y = 0.22\ x + 0.51$	0.42	<0.001
NS	$y = 0.14\ x + 0.53$	0.28	<0.001	$y = 0.16\ x + 0.53$	0.28	<0.001
N	$y = 0.091\ x + 0.53$	0.54	<0.001	$y = 0.11\ x + 0.52$	0.41	<0.001
NI	$y = 0.20\ x + 0.52$	0.27	<0.001	$y = 0.25\ x + 0.51$	0.27	<0.001
TI	$y = 0.20\ x + 0.52$	0.32	<0.001	$y = 0.29\ x + 0.50$	0.47	<0.001

± 6.20% vs. 65.03% ± 5.98%; $P = 0.009$), and N (61.10% ± 4.34% vs. 63.09 ± 5.09%; $P = 0.048$) sectors (Table 2; Fig. 1). Similarly, eyes with MvD_P had a significantly smaller TCA than those without MvD_P in all areas ($P < 0.05$).

A subgroup analysis of 33 eyes with MvD_P of which the largest portion was located only in the TI sector showed significantly lower CVI than those without MvD_P in the TI and T sectors, with sectoral differences highest in the TI (59.11% ± 4.78% vs. 62.95% ± 5.13%; $P < 0.001$), followed by T (62.44% ± 5.37% vs. 65.46% ± 5.56%; $P = 0.023$) sectors (Figs. 1, 2A). Meanwhile, the TCA did not differ between the two groups in any of the areas ($P > 0.05$; Figs. 1, 2B). Because the number of subjects with MvD_P in sectors other than TI was too small ($n = 6$) for statistical analysis, no subgroup analysis was performed for the other subsets.

The linear regression analysis showed a significant positive relationship between CVI and TCA for both groups with and without MvD_P in all areas ($P < 0.05$); r^2 ranged between 0.27 and 0.57 for eyes with MvD_P and between 0.27 and 0.52 for those without MvD_P (Table 3). Meanwhile, the CVI did not have any significant relationship with VF MD, PSD, or RNFL thickness for either group with or without MvD_P in any areas ($P > 0.05$) (Table 4; Fig. 1).

Discussion

The present study used OCT-A to assess the deep-layer microvasculature within βPPA and image binarization of SD-OCT B-scans to assess choroidal vascularity outside βPPA in POAG eyes. Eyes with MvD_P had significantly lower CVI than those without MvD_P in most areas except the TS, NS, and NI sectors. Furthermore, CVI showed a topographic relationship with MvD_P location. These findings suggest that impaired deep-layer microvasculature within βPPA is associated with reduced choroidal vasculature outside βPPA.

Table 4. Linear Regression Analysis of the CVI With VF MD, Pattern Standard Deviation, and RNFL Thickness

	Eyes With MvD_P ($n = 50$)		Eyes Without MvD_P ($n = 50$)	
Variables	r^2	P Value	r^2	P Value
VF MD, dB	0.015	0.403	0.023	0.291
VF PSD, dB	0.004	0.646	0.022	0.308
RNFL thickness, μm				
Global area	0.002	0.786	0.037	0.181
T	0.072	0.060	0.070	0.064
TS	0.018	0.359	0.002	0.733
NS	0.0002	0.926	0.011	0.476
N	0.00002	0.974	0.026	0.262
NI	0.00006	0.957	0.002	0.754
TI	0.060	0.088	0.001	0.796

Evaluation of choroidal vascularity outside βPPA has been problematic until recently. The conventional imaging modality ICG is invasive and of limited use for the provision of images of segmented layers. Despite the recent advent of OCT-A as a noninvasive imaging modality,[3,4,5,7] the choroidal vasculature outside the βPPA is difficult to evaluate due to projection artifacts from the highly reflective vasculature within the RPE.[3,8] In a previous study evaluating the deep-layer microvasculature with ICG and OCT-A, both ICG-determined perfusion defect and OCT-A-determined dropout could be observed only within βPPA.[4] Recently, CVI was introduced to enable the measurement of the choroidal vasculature outside βPPA by means of image binarization of SD-OCT B-scans.[9,11–15] Similarly, recent studies have calculated choroidal vascularity by using SD-OCT images to assess diurnal variation and IOP-related change.[10,17] The present study showed reduced choroidal vasculature outside the βPPA, which corresponded to MvD_P in glaucomatous eyes based on image binarization of SD-OCT. Also, these findings suggest that CVI measurement can serve as a potential noninvasive tool for the quantification of choroidal vasculature in glaucoma.

It is noteworthy that, among the present findings, the TCA was also smaller in eyes with MvD_P than in those without MvD_P, although it did not significantly differ between the two groups in a subgroup analysis of eyes with MvD_P only in the TI sector. Additionally, TCA and CVI were positively correlated in all areas. These findings concur with the notion that thinning of the choroid might originate in vascular insufficiency of the choroidal vasculature.[24–28] Meanwhile, CVI did not show any significant relationship with RNFL thickness, VF MD, or PSD. These findings may add to the literature that choroidal thickness, which may reflect the choroidal vasculature, is not associated with the presence or severity of glaucoma.[28–30] On the other hand, given that the study subjects were matched by age and VF MD according to the main purpose of this study (i.e., to evaluate CVI according to MvD_P), the generalizability of the current results to the general population of glaucoma patients might be limited. Given that the pathogenic role of the choroidal structure in the pathogenesis of glaucoma is controversial,[3,26–33] further studies with large numbers of study subjects are required to better elucidate the relationships among the key factors (i.e., glaucoma severity, choroidal thickness, CVI, and MvD_P).

In the present study, eyes with MvD_P showed a significantly higher prevalence of focal LC defects and a significantly larger BMO area than those without MvD_P. Therefore, the influences of the focal LC defect and a large BMO area on reduced CVI cannot be completely ruled out. However, in the present results, CVI did not have any

significant relationship with VF MD, PSD, or RNFL thickness. Also, it is more likely that CVI is associated with focal LC defect indirectly through the MvD_P than directly, because βPPA is closer to the LC than the choroid outside the βPPA. Meanwhile, a large BMO area of eyes with MvD_P might lead to a falsely thin choroid compared with those without MvD_P, because the choroid is reported to be thickest in the macula and to decrease toward the peripapillary lesion.[34] However, the TCA values of the eyes with MvD_P were lower than those without MvD_P. Therefore, TCA differences between the two groups would become smaller after adjusting for BMO area. In any case, given that the CVI is the proportion of the choroidal vascularity relative to the total choroidal tissue at the same point, the influence of the measurement point on the CVI would not be remarkable.

The present study has several limitations. First, there was a CVI overlap between eyes with and without MVD_P. This might have been partly due to the limitation of the current CVI technique, which does not allow for isolation of the choriocapillaris.[10] Thus, the medium or large choroidal vessels that might not be affected by the MvD_P were included in the derivation of the CVI. If isolation of the choriocapillaris becomes possible, the differences between eyes with and without MvD_P might become more noticeable. Second, the CVI was derived by a novel technique based on image binarization of the intensity of the choroidal tissue on SD-OCT B-scans. The clinical utility of this method is uncertain, due to lack of a noninvasive gold standard for determination of choroidal vascularity outside the βPPA. Also, this technology itself has several technical limitations: (1) the possibility of falsely high CVI measurement due to shadowing of the large superficial retinal vessels, (2) the limitations of the current technique for accurately isolating the choriocapillaris, and (3) the lack of adjustment of ocular magnification for calculation of TCA and CVI.[10] However, according to our data, age, RNFL thickness, CCT, and the axial length of eyes with and without MvD_P did not differ significantly. These findings suggest that the diameters and radial distribution of the large superficial retinal vessels,[35] as well as the influence of ocular magnification on the TCA, would not differ significantly between the two groups Moreover, CVI would not be influenced by axial length, because it is computed by dividing the LA by the TCA, both of which are equally affected by ocular magnification. Furthermore, these limitations have been at least partially addressed by a number of studies using the current image binarization technique for both normal subjects and various retinal diseases.[10,11,13,14] In any case, improvement and validation of this technique is needed.

In conclusion, eyes with MvD_P had a significantly lower CVI than those without MvD_P. Furthermore, reduced CVI was spatially correlated with MvD_P. These findings suggest that deep-layer microvasculature dropout within the βPPA is associated with reduced choroidal microvasculature outside the βPPA. Further longitudinal studies on the temporal relationship between reduced choroidal vasculature outside the βPPA and deep-layer microvasculature dropout within the βPPA are warranted.

Acknowledgments

The authors thank Hae Rang Kim, MD, for her data acquisition.

Disclosure: **J.W. Park**, None; **M.H. Suh**, None; **R. Agrawal**, None; **N. Khandelwal,** None

References

1. Flammer J. The vascular concept of glaucoma. *Surv Ophthalmol*. 1994;(38 suppl):S3–S6.
2. Weinreb RN. Ocular blood flow in glaucoma. *Can J Ophthalmol*. 2008;43:281–283.
3. Suh MH, Zangwill LM, Manalastas PI, et al. Deep retinal layer microvasculature dropout detected by the optical coherence tomography angiography in glaucoma. *Ophthalmology*. 2016; 123:2509–2518.
4. Lee EJ, Lee KM, Lee SH, Kim TW. Parapapillary choroidal microvasculature dropout in glaucoma: a comparison between optical coherence tomography angiography and indocyanine green angiography. *Ophthalmology*. 2017;124: 1209–1217.
5. Akagi T, Iida Y, Nakanishi H, et al. Microvascular density in glaucomatous eyes with hemifield visual field defects: an optical coherence tomography angiography study. *Am J Ophthalmol*. 2016;168:237–249.
6. Suh MH, Zangwill LM, Manalastas PI, et al. Optical coherence tomography angiography vessel density in glaucomatous eyes with focal lamina cribrosa defects. *Ophthalmology*. 2016;123: 2309–2317.
7. Lee EJ, Kim TW, Kim JA, Kim JA. Parapapillary deep-layer microvasculature dropout in primary open-angle glaucoma eyes with a parapapillary gamma-zone. *Invest Ophthalmol Vis Sci*. 2017;58:5673–5680.
8. Lee EJ, Kim S, Hwang S, Han JC, Kee C. Microvascular compromise develops following nerve fiber layer damage in normal-tension glaucoma without choroidal vasculature involvement. *J Glaucoma*. 2017;26:216–222.
9. Agrawal R, Gupta P, Tan KA, Cheung CM, Wong TY, Cheng CY. Choroidal vascularity index as a measure of vascular status of the choroid: measurements in healthy eyes from a population-based study. *Sci Rep*. 2016;6:21090.
10. Zhang X, Cole E, Pillar A, et al. The effect of change in intraocular pressure on choroidal structure in glaucomatous eyes. *Invest Ophthalmol Vis Sci*. 2017;58:3278–3285.
11. Wei X, Ting DSW, Ng WY, Khandelwal N, Agrawal R, Cheung CMG. Choroidal vascularity index: a novel optical coherence tomography based parameter in patients with exudative age-related macular degeneration. *Retina*. 2017;37:1120–1125.
12. Agrawal R, Chhablani J, Tan KA, Shah S, Sarvaiya C, Banker A. Choroidal vascularity index in central serous chorioretinopathy. *Retina*. 2016;36:1646–1651.
13. Agrawal R, Li LK, Nakhate V, Khandelwal N, Mahendradas P. Choroidal vascularity index in Vogt-Koyanagi-Harada disease: an EDI-OCT derived tool for monitoring disease progression. *Trans Vis Sci Tech*. 2016;5(4):7.
14. Agrawal R, Salman M, Tan KA, et al. Choroidal vascularity index (CVI)—a novel optical coherence tomography parameter for monitoring patients with panuveitis? *PLoS One*. 2016; 11:e0146344.
15. Ng WY, Ting DS, Agrawal R, et al. Choroidal structural changes in myopic choroidal neovascularization after treatment with antivascular endothelial growth factor over 1 year. *Invest Ophthalmol Vis Sci*. 2016;57:4933–4939.
16. Tan KA, Laude A, Yip V, Loo E, Wong EP, Agrawal R. Choroidal vascularity index—a novel optical coherence tomography parameter for disease monitoring in diabetes mellitus? *Acta Ophthalmol*. 2016;94:e612–e616.
17. Kinoshita T, Mitamura Y, Shinomiya K, et al. Diurnal variations in luminal and stromal areas of choroid in normal eyes. *Br J Ophthalmol*. 2017;101:360–364.
18. Suh MH, Park JW, Kim HR. Association between the deep-layer microvasculature dropout and the visual field damage in glaucoma. *J Glaucoma*. 2018;27:543–551.
19. Park SC, Hsu AT, Su D, et al. Factors associated with focal lamina cribrosa defects in glaucoma. *Invest Opthalmol Vis Sci*. 2013;54:8401–8407.

20. Kiumehr S, Park SC, Dorairaj S, et al. In vivo evaluation of focal lamina cribrosa defects in glaucoma. *Arch Ophthalmol*. 2012;130:552–559.
21. Sonoda S, Sakamoto T, Yamashita T, et al. Choroidal structure in normal eyes and after photodynamic therapy determined by binarization of optical coherence tomographic images. *Invest Ophthalmol Vis Sci*. 2014;55:3893–3899.
22. Sonoda S, Sakamoto T, Yamashita T, et al. Luminal and stromal areas of choroid determined by binarization method of optical coherence tomographic images. *Am J Ophthalmol*. 2015;159:1123–1131.e1.
23. Niblack W. *An Introduction to Digital Image Processing*. Englewood Cliffs, New Jersey: Prentice Hall International Inc., 1986:112–128.
24. Sullivan-Mee M, Patel NB, Pensyl D, Qualls C. Relationship between juxtapapillary choroidal volume and beta-zone parapapillary atrophy in eyes with and without primary open-angle glaucoma. *Am J Ophthalmol*. 2015;160:637–647.
25. Lee SH, Lee EJ, Kim TW. Topographic correlation between juxtapapillary choroidal thickness and microstructure of parapapillary atrophy. *Ophthalmology*. 2016;123:1965–1973.
26. Lee KM, Lee EJ, Kim TW. Juxtapapillary choroid is thinner in normal-tension glaucoma than in healthy eyes. *Acta Ophthalmol*. 2016;94:e697–e708.
27. Van Keer K, Abegao Pinto L, Willekens K, Stalmans I, Vandewalle E. Correlation between peripapillary choroidal thickness and retinal vessel oxygen saturation in young healthy individuals and glaucoma patients. *Invest Ophthalmol Vis Sci*. 2015;56:3758–3762.
28. Ehrlich JR, Peterson J, Parlitsis G, et al. Peripapillary choroidal thickness in glaucoma measured with optical coherence tomography. *Exp Eye Res*. 2011;92:189–194.
29. Li L, Bian A, Zhou Q, Mao J. Peripapillary choroidal thickness in both eyes of glaucoma patients with unilateral visual field loss. *Am J Ophthalmol*. 2013;156:1277–1284.
30. Maul EA, Friedman DS, Chang DS, et al. Choroidal thickness measured by spectral domain optical coherence tomography: factors affecting thickness in glaucoma patients. *Ophthalmology*. 2011;118:1571–1579.
31. Hirooka K, Tenkumo K, Fujiwara A, Baba T, Sato S, Shiraga F. Evaluation of peripapillary choroidal thickness in patients with normal-tension glaucoma. *BMC Ophthalmol*. 2012;12:29.
32. Park HY, Lee NY, Shin HY, Park CK. Analysis of macular and peripapillary choroidal thickness in glaucoma patients by enhanced depth imaging optical coherence tomography. *J Glaucoma*. 2014;23:225–231.
33. Lee SH, Lee EJ, Kim TW. Topographic correlation between juxtapapillary choroidal thickness and parapapillary deep-layer microvasculature dropout in primary open-angle glaucoma. *Br J Ophthalmol*. 2017;11:e311136.
34. Zhang C, Tatham AJ, Medeiros FA, Zangwill LM, Yang Z, Weinreb RN. Assessment of choroidal thickness in healthy and glaucomatous eyes using swept source optical coherence tomography. *PLoS One*. 2014;9:e109683.
35. Chung HJ, Park CK. Factors determining the peripapillary retinal nerve fiber distribution. *J Glaucoma*. 2014;23:471–476.

Investigative Ophthalmology & Visual Science